Advances in Military Technology
Vol. 20, No. 2, 2025, pp. 483-496
ISSN 1802-2308, eISSN 2533-4123
DOI 10.3849/aimt.01991

Research on the Reflectivity of Lens Air Target Simulators

H. Ivanets[1], S. Horielyshev[3*], M. Ivanets[2], A. Nakonechnyi[1], V. Voinov[1], O. Stavytskyi[1], A. Galuzinskyi[1], L. Khrol[1], and O. Serhiienko[3]

[1]*Ivan Kozhedub Kharkiv National Air Force University, Kharkiv, Ukraine*
[2]*State Scientific Research Institute of Armament and Military Equipment Testing and Certification, Cherkasy, Ukraine*
[3]*National Academy of National Guard of Ukraine, Kharkiv, Ukraine*

The manuscript was received on 11 April 2025 and was accepted after revision for publication as an original research paper on 24 October 2025.

Abstract:

To simulate air targets of various types in the ultrahigh frequency radar range, multilayer spherical Luneberg lenses have become widely used. The reflective properties of such lenses depend on both their absolute dimensions and irradiation frequency, and on the properties of the dielectric material, design features, and their manufacturing technology. This research considers six-layer spherical Luneberg lenses with their uniform division into layers by dielectric permittivity. The calculations performed have shown that the average absolute error in the approximation of the dielectric permittivity to the theoretical law of change when the lens is uniformly divided into six layers by dielectric permittivity is no more than 6.8 %. Theoretical calculations and experimental studies have revealed the influence of the design features of spherical lenses, the characteristics of the dielectric material, and the features of the manufacturing technology on the reflective properties of such air target simulators.

Keywords:

reflective properties, radar cross section, Luneberg lens, dielectric material, design features, manufacturing technology

1 Introduction

In the USA, Great Britain, and other leading European countries, unmanned aerial vehicles (UAVs) equipped with multilayer spherical Lüneberg lenses (LLs) have become widely used for passive simulation of various types of aerial targets in the ultra-high frequency radar range [1-3].

[*] *Corresponding author: Scientific and Research Center of Service and Military Activities of the National Guard of Ukraine, Kharkiv, National Academy of National Guard of Ukraine, Zakhysnykiv Ukrainy sq., 3, Ukraine. Phone: +380 67 959 91 53, E-mail: port_6633@ukr.net*

The purpose of such lenses is to increase the radar cross section (RCS) by several tens of times, thus simulating more significant targets [4]. The advantages of such UAVs with LL are both cheapness and ease of manufacture. Multilayer spherical LL is a dielectric sphere of arbitrary size, capable of converting a spherical wavefront into a flat one. To do this, it must provide a smooth decrease in the dielectric constant of the lens material from the center to its edge. It is quite difficult to manufacture a classical LL with a continuous law of change in the dielectric constant (refractive index) along its radius.

The reflective properties of spherical LLs, which are used as air target simulators, depend on both their absolute dimensions and irradiation frequency, as well as the properties of the dielectric material, design features and their manufacturing technology. When manufacturing such reflectors in the form of multilayer structures, the discreteness of the change in dielectric permittivity and additional design errors lead to a deterioration in their reflective properties compared to the theoretical value.

Thus, there is a need to study the influence of the properties of the dielectric material, design features, and manufacturing technology of spherical LLs on their "reflective" properties as passive RCS simulators of air targets.

Modern research on the use of various dielectric materials and the comparison of their properties, design features, manufacturing technology and application of spherical LLs as passive simulators of air targets is covered in a number of works. Thus, in work [4] it is stated that foam dielectric materials can be used as a material for the manufacture of spherical LLs, the refractive index of which depends on the density, for example, polystyrene foam, polystyrene, etc. In addition, various dielectric composite materials with good technological properties can be used. Such materials include synthetic polymers and dielectric substances, for example, ceramic powders. Composite materials have a low weight and good dielectric properties. Therefore, their use allows you to create various designs of spherical LLs.

In works [5-8], spherical LLs manufactured using various three-dimensional printing technologies are described. Thus, in work [5] an approach to creating a pherical LL with radial holes is presented. The study investigated how the dielectric constant and loss tangent of equivalent lens materials are influenced by hole shape, orientation, and porosity. However, using this technology, LLs were created with only two layers, which does not allow to fully reduce the discreteness of the changes in the dielectric constant.

The authors of [6] proposed a low gain LL antenna of 20 dB using the 3D printing concept. The required continuous permittivity law was implemented by varying the size of dielectric cubes centered at the joints of a plastic rod.

And in [7], a new method for creating antennas from LLs is presented, which combines the production of a fused filament by additive manufacturing technology with an effective media approach that uses space-filling curves. Two LLs were created, which are designed to operate in separate frequency ranges (26–40 GHz and 70–110 GHz) with antenna gains of 20 and 24 dB, respectively.

Important aspects of designing and implementing electromagnetic (EM) components through 3D printing based on polymer inkjet printing are highlighted in [8]. A number of polymer materials, their broadband EM characteristics in the GHz to THz range, and a methodology for designing 3D printed antennas and other electromagnetic components are presented.

But these approaches to creating LLs using three-dimensional printing have some disadvantages, such as limited dimensions of the printed product and fairly high cost of

equipment and materials. Moreover, they require a detailed study of the manufacturing technology.

The authors of the article [9] considered various and quite original options for manufacturing LLs, but most of them implement a stepwise approximation of the refractive index to the required law of change, i.e. the lens is implemented in the form of a multilayer material with different dielectric constant parameters. As a rule, the dielectric constant inside each layer is constant and varies discretely from layer to layer. The authors note that the implementation of LLs with the number of layers higher than 10 is impractical and does not lead to significant changes in the characteristics of the lens. In practice, 4–6-layer lenses have the greatest manufacturability.

In [10], the possibilities of manufacturing LLs by printing on a 3D printer using the technology of jet polymerization, which includes electromagnetic crystals in the structure, were analyzed. In order to create LLs with the required refractive index, it is necessary to use a non-uniform dielectric as the main material of the lens body. The parameters of the dielectric can be changed if the density of its filling is controlled during 3D printing. In this case, the dielectric constant of the material should vary in a narrow range: from two in the center to one on the surface.

References [3, 11-13] examine various methods for simulating the radar cross section (RCS) of targets, including corner reflectors, self-focusing antenna arrays, Lüneberg lenses (LLs), and two-point coupled simulators. The comparative analysis showed that simulators based on LL of different designs have the highest RCS and allow to cover the entire radar wavelength range. In addition, the use of LL allows to simulate the RCS of most modern air targets (aircraft, cruise missiles and others).

Thus, the analysis of the literature indicates that while the influence of dielectric materials, design features, and manufacturing technologies on the reflective properties of multilayer spherical Lüneberg lenses (LLs) – as key components of passive RCS simulators for aerial targets – is a relevant topic, it remains insufficiently studied. The purpose of the article is to study the influence of dielectric material, design features, and manufacturing technology on the "reflective" properties of spherical LLs as passive air target simulators.

To achieve this aim, it is necessary to solve the following tasks:

- to conduct theoretical studies of the influence of the design features of spherical lens simulators of air targets on their reflective properties,
- to conduct experimental studies on the influence of dielectric material, design and manufacturing technology on the reflective properties of spherical air target simulators.

2 Theoretical Studies of the Influence of Design Features of Spherical Lens Simulators of Air Targets on Their Reflective Properties

The reflectivity of an air target simulator is a measure of the ability of the simulator surface to reflect electromagnetic radiation [14]. The main characteristic of the reflectivity of any target is the RCS, which is completely determined by the power of electromagnetic energy reflected by the target in the direction of the radar receiver. The defining element of all lens simulators of air targets are dielectric lenses of various types.

Most often, certain modifications of spherical dielectric LLs are used. These lenses are a multilayer sphere with different values of the dielectric permittivity of the layers and, accordingly, their refractive indices [15]. The dielectric permittivity of an ideal LL

without loss smoothly changes along the radius of the sphere from $\varepsilon = 1$ on the surface of the lens to $\varepsilon = 2$on the axis of the lens according to the law:

$$\varepsilon(a) = 2 - \left(\frac{a}{r}\right)^2 \tag{1}$$

where r – the lens radius, a – the radial coordinate of an arbitrary point inside the lens.

The radial coordinate of an arbitrary point will be comprehended as the distance from the center of the lens to this point along the radius of the lens.

The form of the law Eq. (1) of the change in dielectric constant from the normalized radial coordinate of the lens is presented in Fig. 1.

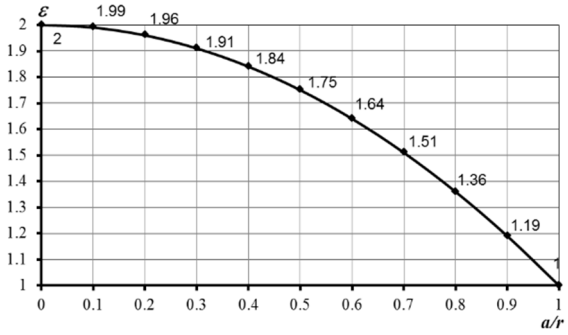

Fig. 1 View of the law of change of dielectric permittivity from normalized radial coordinate of lens

We assume that the radius of the lens is much larger than the wavelength of the radiation. This means that at distances of the order of the wavelength of the radiation, the dielectric constant changes very little. In this case, the refractive index [16] is:

$$n(a) = \sqrt{\varepsilon(a)} = \sqrt{2 - \left(\frac{a}{r}\right)^2} \tag{2}$$

where $n(a)$ – the refractive index.

In an inhomogeneous medium, where the refractive index is a function of coordinates, the beam bends in the direction of increasing refractive index. Accordingly, all rays, regardless of the angle of incidence on the lens surface, have the same phase lengths and converge at one-point F (focus), which lies on the lens surface on the opposite side of it. With small deviations from the law of change of dielectric constant Eq. (1) the position of the lens focus shifts along the direction of wave incidence either inside the lens or behind it.

To turn an LL into a reflector, it is enough to place a metal plate at its focus. As a rule, this is achieved by metallizing part of the lens surface. Due to symmetry, the rays incident on the plate and those reflected from it follow identical paths and, upon exiting the lens, propagate in the opposite direction, forming a planar phase front.

This study considers spherical passive dielectric target simulators, which are built on the basis of spherical dielectric LLs [7, 13, 15]. The reflector is a larger inhomogeneous dielectric sphere compared to the wavelength, part of which is metallized in the form of a “cap” (segment). The reflection of an electromagnetic wave

in a dielectric sphere occurs from the metallized surface. The shape of the metallized surface determines the scattering indicator of the spherical LL. The maximum monostatic RCS [3, 13, 16] created by a metallized spherical lens in the form of a "cap" is determined by the aperture method according to the formula:

$$\sigma_1 = 4\frac{\pi^3 r^4 f^2}{c^2} \tag{3}$$

where σ_1 – the maximum monostatic RCS of a spherical LL with a metallized segment in the form of a "cap", f – the frequency of the electromagnetic wave of radiation, c – the speed of light.

The monostatic scattering indicatrix of the simulator is a body of revolution with an axis passing through the center of the lens and the center of the metal "cap". The shape of the indicatrix depends on the angular size of the "cap" and is determined on the basis of a geometric construction considering the "darkening" created by the "cap" at large angles of deviation of the line of sight from the axis of the reflector (simulator). From Eq. (3) it follows that the RCS of such a lens depends on both the radius of the lens itself and the frequency of the electromagnetic wave of irradiation.

If a spherical air target lens simulator has a metallized "cap," it provides a scattering indicatrix of about 170° in both planes. Design complications allow the indicatrix to be expanded even further and circular directivity to be obtained in one of the planes, but at the expense of reducing the RCS and narrowing the indicatrix in the other plane.

LL designs may differ from each other in the shape of the metallized surface. Instead of a segmented "cap", a continuous equatorial belt with a width of h, which leads to the effect of "shading", the effect of which reduces the RCS (reflective properties of the lens). In this case, the maximum monostatic numerical value of the RCS of a LL with a continuous equatorial belt is σ_2, is expressed by the formula [13]:

$$\sigma_2 = 4\frac{\pi^3 r^4 f^2}{c^2}\cdot\left(1-\frac{2h}{\pi r}\right)^2 = \sigma_1\left(1-\frac{2h}{\pi r}\right)^2 \tag{4}$$

where h– the width of the continuous equatorial belt.

Fig. 2 shows the dependence of the normalized monostatic RCS (σ_2/σ_1) from the ratio of the width of the continuous equatorial belt and the radius of the lens (h/r) from 0 to 3.14, i.e. until the lens surface is completely metallic [13].

Analysis of the obtained data (Fig. 2) shows that the design of a spherical LL significantly affects the reflective properties of an air target simulator. Thus, the RCS of target simulators based on LL with a metallized segment in the form of a "cap" significantly exceeds the RCS of simulators based on LL with a solid equatorial belt.

At the same time, the maximum monostatic value of the RCS created by LL with a solid equatorial belt depends on the ratio h/r. It is advisable to consider only those simulators with LL in the presence of a continuous equatorial belt for which the ratio h/r does not exceed 0.3925. In addition, it should be noted that a spherical LL turns into a reflector (air target simulator) only in the case when part of the dielectric sphere in the form of a segment (or "cap" or a solid equatorial belt) is metallized.

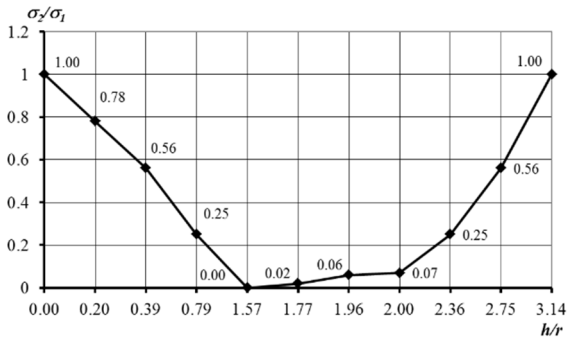

Fig. 2 Dependence of normalized monostatic RCS on h/r

Since the manufacture of spherical LLs with a smooth change in dielectric constant along the radius Eq. (1) is a rather complex task, in practice they proceed to a stepwise approximation of the law of change in dielectric constant using a multilayer structure. According to [9], the optimal LL design consists of six layers. The following methods of dividing the lens into layers are distinguished [17]: uniform division by refractive index; uniform division of the lens by dielectric constant; uniform division of the lens by radius. In this work, six-layer LLs with uniform division into layers by dielectric constant are considered. The essence of uniform division of the lens into layers by dielectric constant is as follows. The dependence of the dielectric constant on the radius is divided into equal parts by $\varepsilon(a)$. The corresponding layer radii are found $a_1, a_2, \ldots, a_{N-1}, a_N = r$. Each layer is divided into two equal parts. The dielectric constant is taken equal to the average in each layer of the lens, i.e. $\varepsilon_i' = \varepsilon\left[a_{i-1} + 0,5\left(a_i - a_{i-1}\right)\right]$. Thus, we obtain a uniform partition by dielectric permittivity (by $\varepsilon(a)$). Such an approximation function allows us to approximate the change in dielectric permittivity to the smooth law Eq. (1) due to the change in the dielectric filling density in the lens structure.

The algorithm for dividing the LL into layers by dielectric constant is shown in Fig. 3. The parameters of the LL layers when the lens is evenly divided into layers by dielectric constant are given in Tab. 1. The appearance of the LL and their cross-section are shown in Fig. 4.

The closer the permittivity distribution law approaches continuous, the less the characteristics of the multilayer lens differ from the ideal LL. As a criterion for the effectiveness of the stepwise approximation of the permittivity change law to the theoretical one, we have chosen the average absolute error of approximation, which is calculated as follows:

$$\delta = \frac{\sum_{i=1}^{N}\sum_{k=1}^{K_i}\left|\varepsilon_i' - \varepsilon_{ik}\right|}{K} \tag{5}$$

where δ – the average absolute error of approximation,

ε_i' – the value of the dielectric constant for the i-th layer of the LL,

ε_{ik} – theoretical values of dielectric permittivity in the ith layer of the LL,

K_i – the number of dielectric constant values to be analyzed in i-th at layer of LL,

$K = \sum_{i=1}^{N} K_i$ – the total number of dielectric permittivity values of the LL to be analyzed.

The calculations of Eq. (5) showed that the average absolute error of the approximation of the dielectric constant to the theoretical law of change with a uniform division of the LL into layers by dielectric constant is no more than 0.06745 (6.8 %).

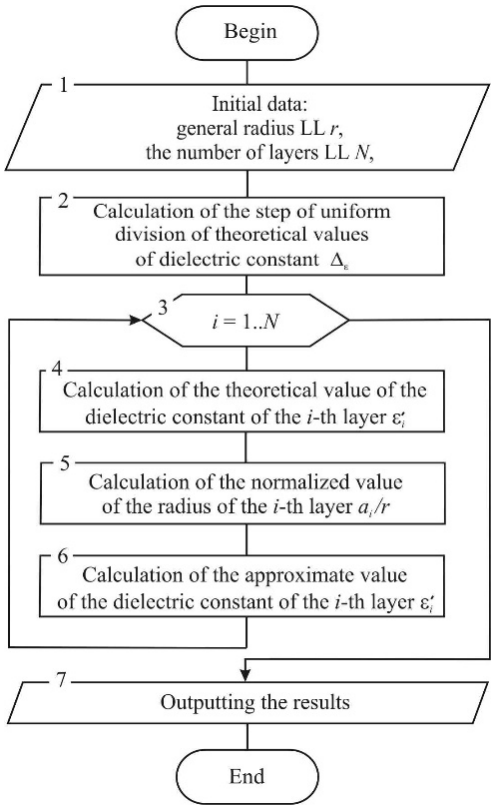

Fig. 3 Algorithm for uniform division of the LL into layers by dielectric constant

a) b)

Fig. 4 Appearance of LL (a) and their cross section (b)

3 Experimental Study of Dielectric, Design, and Manufacturing Effects on Reflective Properties of Spherical Air Target Simulators

Experimental studies were conducted to study the influence of dielectric material and design features on the "reflective" properties of lens simulators. The following lens simulators were used:

- two six-layer spherical LLs with cubic holes made of dielectric material such as PLA using 3D printing technology, radius $r = 97$ mm with and without a metallized segment in the form of a "cap",
- two six-layer spherical LLs with cubic holes of radius $r = 45$ mm with a metallized segment in the form of a "cap", made using 3D printing technology from various dielectric materials (PET and PETG).

The following dielectric materials were used to manufacture spherical LLs:

- *Polylactide PLA* – one of the most widely used environmentally friendly thermoplastics. PLA is a polymer of lactic acid, which easily absorbs water and is relatively soft. It is a colorless transparent material, the density of which is 1.22–1.25 kg/dm^3. One of the most important factors for the use of PLA in 3D printing is its low melting point 170–180 °C, which contributes to a relatively low electricity consumption. However, PLA solidifies quite slowly, as the glass transition temperature is 50–58 °C. The dielectric loss of PLA is in the range of 2.3–2.6 [18].
- *Dielectric materials such as PET and PETG.* Polyethylene terephthalate glycol (PETG) is a thermoplastic polyester that provides high chemical resistance and durability. PETG is an adaptation of PET (polyethylene terephthalate), where "G" stands for glycol. PETG has a greater strength and durability, is more impact resistant, and is better suited to higher temperatures. Due to the low molding temperatures of PETG, it is easy to vacuum and pressure mold or bend. PETG is a transparent, amorphous material with a glass transition temperature of 80–85 °C and a melting point ranging from 180 to 230 °C. Its density falls between 1.26 and 1.28 kg/dm³. The dielectric constant of PETG ranges from 2.81 to 3.30 [18]. Unlike PETG, PET-type plastic is prone to crystallization at high temperatures, which makes it opaque and weakens its structure.

Experimental studies were carried out in an anechoic chamber. Fig. 5 shows the equipment of the measuring stand, which includes: transmitting and measuring antennas, a laser level (Fig. 5a), as well as a portable vector circuit analyzer (FieldFox microwave analyzer) (Fig. 5b).

A vector network analyzer (VNA) measures the characteristics of the signal passing through the test device and the characteristics of the signal reflection from its ports (S-parameters) [19]. For two-port devices, the reflection characteristic from the first port is defined as S11, the forward transmission characteristic is S21, the reverse transmission characteristic is S12, and the reflection characteristic from the second port is S22 (Fig. 6). Each S-parameter contains an amplitude-frequency and a phase-frequency characteristic.

The experiment was carried out in the S12 VNA characteristic measurement mode using frequency domain filtering. The LLs were irradiated by a horn antenna connected to port 1 of the VNA via a coaxial cable using coaxial wave transitions (CWT). A broadband horn antenna of the P6-223 type was used as a measuring antenna connected to port No. 2 of the VNA via a flexible coaxial cable using CWT. The LLs

were placed in the BEC on a stand made of polystyrene panels and oriented relative to the geometric axes of the antennas using a laser level (Fig. 5a). The distance between the antennas and the LLs under study was 1.5 m, which is the far zone for LLs of this size.

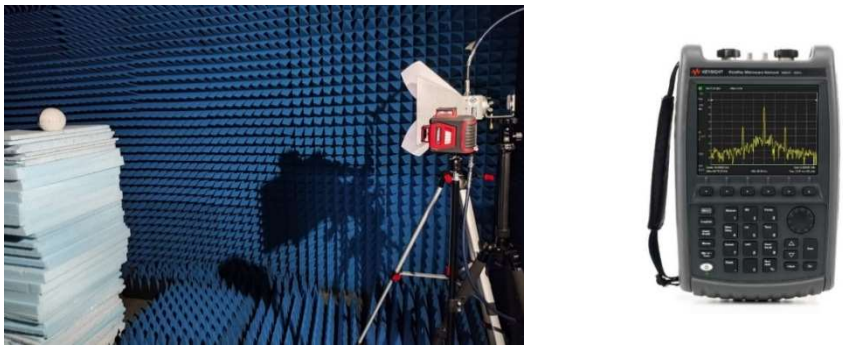

a) *b)*

Fig. 5 Equipment of measuring stand. a) transmitting, measuring antennas and laser level; b) Keysight N9951A – portable microwave analyzer Field Fox

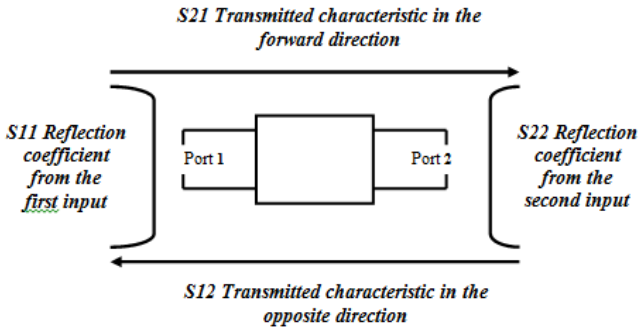

Fig. 6 S*-parameters of vector circuit analyzer*

Key technical specifications and capabilities of the FieldFox portable microwave analyzer are as follows: its frequency range is from 5 kHz to 44 GHz; it includes an antenna-feeder device analyzer; it has options for a vector circuit analyzer, spectrum analyzer, power meter, and vector voltmeter.

VNA allows you to simultaneously measure distances to inhomogeneities and reflection parameters and simultaneously measure all four S-parameters.

Minimum distance $R_{\min}$ to LL when measuring [19] is determined in accordance with the expression:

$$R_{\min} = \frac{\pi D^2}{4\Delta\varphi\lambda} \tag{6}$$

where $\Delta\varphi = \pi/8$ – the maximum phase error at the edge of the standard under investigation, D – the diameter of spherical LL.

During the experiment, the power of the reflected electromagnetic wave from two lenses at the receiver input was compared with the transmitter power in decibels:

$$\left.\begin{aligned} P_1[\mathrm{dB}] &= 10\log(P_1/P_0) \\ P_2[\mathrm{dB}] &= 10\log(P_2/P_0) \end{aligned}\right\} \quad (7)$$

where P_1 – the power of the received signal reflected from the first lens,

P_2 – the power of the received signal reflected from the second lens,

P_0 – the transmitter power.

The difference in relative power of received signals in decibels ΔP[dB] proportional to the ratio of the powers of the signals reflected by the lenses is computed as follows:

$$\Delta P[\mathrm{dB}] = P_1[\mathrm{dB}] - P_2[\mathrm{dB}] = 10\log(P_1/P_0) - 10\log(P_2/P_0) = 10\log(P_1/P_2) \quad (8)$$

The difference in the relative powers ΔP[dB] of the reflected signals from two LLs allows us to compare the reflective capabilities of the lenses under investigation. A positive difference in powers, taking into account its magnitude, indicates the advantages of the reflective properties of the first LL over the second. A negative difference in powers, taking into account its magnitude, indicates the advantages of the reflective properties of the second LL over the first.

Initially, two six-layer LLs of the same radius (r = 97 mm) were made of PLA dielectric using 3D printing technology. The difference in the design of the lenses was that the first lens had a metallized segment in the form of a "cap" (a hemisphere wrapped in foil), and the second without it. Fig. 7 shows the frequency dependences of the relative radiation power of the first and second lenses at the receiver input in the X-frequency range (from 8 to 12 GHz inclusive).

The frequency dependence of the difference in relative powers ΔP[dB] of the first and second lenses under investigation is shown in Fig. 8.

Analysis of the obtained results (Figs 7-8) shows that the LL without a metallized segment in the form of a "cap" (the second sphere) has rather weak reflective properties.

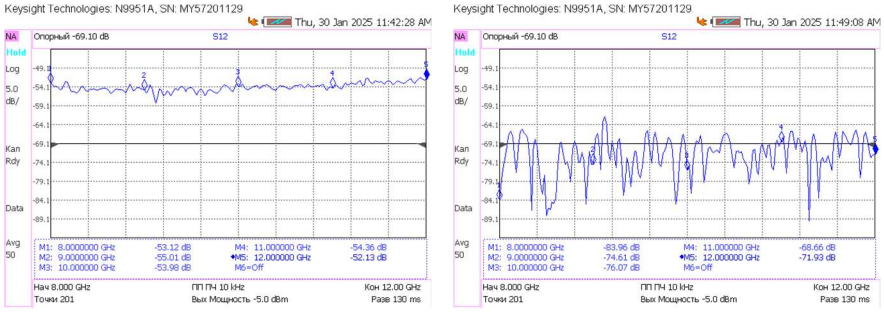

a) *b)*

Fig. 7 Frequency dependence of relative radiation power of LL. a) half-wrapped with foil; b) not wrapped with foil

The LL with a metallized segment (foil) in the form of a "cap" (the first sphere) has very good reflective properties and surpasses the second one in the X-band of frequencies from 3.49 to 36.99 dB (i.e. from 2 to 5 000 times). This confirms the fact that for the use of a spherical LL as an air target simulator, a necessary condition is the metallization of a part (segment) of the lens.

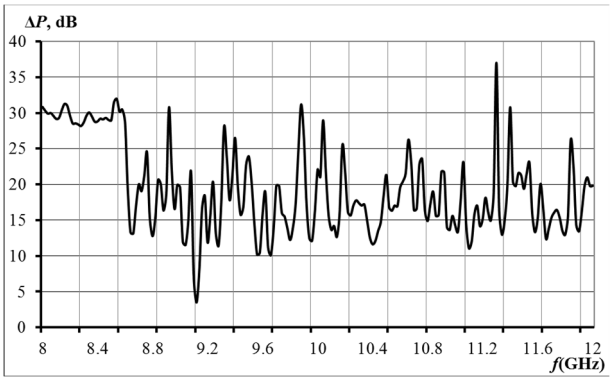

Fig. 8 Frequency dependence of difference in decibels of relative radiation power of the first and second LL

During the experimental study, two six-layer Luneburg lenses (LL) with metallized "cap" segments of identical radius ($r = 45$ mm) were compared. Both lenses were fabricated using 3D printing technology. The first LL was made of polyethylene terephthalate glycol (PETG), while the second used polyethylene terephthalate (PET).

The frequency dependences of the relative radiation power of the first and second lenses at the receiver input are shown in Fig. 9.

The frequency dependence of the difference in relative powers ΔP[dB] of the first and second lenses under investigation is shown in Fig. 10.

Analysis of the obtained results (Figs 9-10) showed the following. The reflective properties of LLs depend on both the dielectric material from which they are made and the frequency of irradiation.

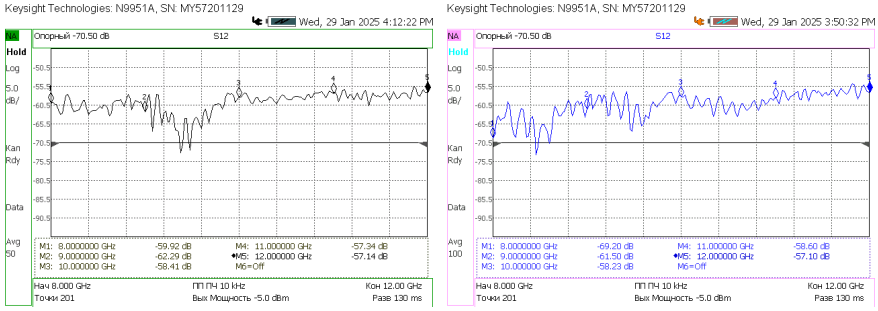

a) *b*)

Fig. 9 Frequency dependence of relative radiation power of a LL with a metallized segment in the form of a "cap". a) PETG material; b) PET material

In some frequency ranges (especially in the 8–9 GHz, 10.2–11.0 GHz ranges), the reflective properties of a lens made of dielectric material such as PETG exceed the reflective properties of lenses made of dielectric material such as PET by an amount from 0.1 to 11.9 dB, while in other frequency ranges (especially in the 9–10 GHz ranges) the situation is the opposite – a lens made of dielectric material such as PET exceeds the reflective properties of a lens made of dielectric material such as PETG by an amount from 0.1 to 13 dB.

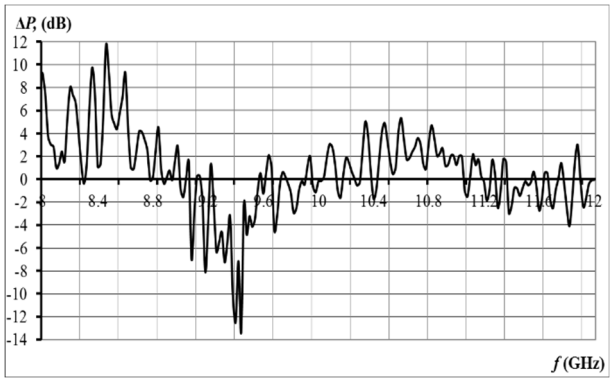

Fig. 10 Frequency dependence of difference in decibels of relative radiation power of the first (PETG) and second (PET) LL with metallized segments in the form of a "cap"

Thus, the analysis of the obtained theoretical and experimental studies showed that:

- a necessary condition for converting dielectric LLs into air target simulators is the presence of a metallized part (segment) of the lens, otherwise it has rather weak reflective properties and its use as a simulator is impractical,
- the reflective properties of such LLs depend on both their absolute dimensions and irradiation frequency, as well as the dielectric material, design features, and their manufacturing technology,
- comparisons of the reflective properties of lenses made from different dielectric materials have shown that at some frequencies, the reflective properties of lenses made from one dielectric material exceed the reflective properties of lenses made from another dielectric material, while at other frequencies the situation is the opposite.

4 Conclusions

Spherical passive dielectric air target simulators are created on the basis of dielectric spherical LLs. To transform the LL into a reflector, it is necessary to metallize part of the dielectric sphere (segment). The designs of such lenses differ from each other in the shape of the metallized surface: with a metallized surface in the form of a "cap" or with a continuous equatorial belt of a certain width.

The reflective properties of spherical LLs, which are used as air target simulators, depend on both their absolute dimensions and irradiation frequency, and on the dielectric material, design features and technology of their manufacture. When manufacturing spherical reflectors in the form of multilayer LLs, the discreteness of the change in dielectric constant and additional design errors lead to a deterioration of their reflective properties in comparison with the theoretical value by 2–3 dB. The closer the dielectric constant distribution approaches continuity, the more closely the characteristics of the multilayer lens resemble those of the ideal lens.

There are the following ways of dividing a spherical LL into layers: uniform division by refractive index; uniform division of the lens by dielectric constant; uniform division of the lens by radius. In this work, six-layer LLs with uniform division into layers by dielectric constant were considered. The calculations performed showed that the average absolute error of the approximation of the dielectric constant to the

theoretical law of change with uniform division of the LL into six layers by dielectric constant is no more than 6.8 %.

Theoretical calculations and experimental studies have confirmed that the design features of spherical LLs (the shape of the metallized surface), dielectric material and manufacturing technology significantly affect their reflective properties. Thus, the reflective properties of spherical simulators based on LLs with a metallized surface in the form of a segmented "cap" exceed the reflective properties of simulators based on LLs with a solid equatorial belt, which is explained by the effect of the "shading" effect. A comparison of the reflective properties of lenses made from different dielectric materials revealed that, at certain frequencies, lenses composed of one material may exhibit superior reflective performance compared to those made from another. However, at other frequencies, the opposite may be true. Therefore, when designing air target simulators, it is essential to consider the operating frequencies of the adversary's electronic reconnaissance systems.

Acknowledgement

The work presented in this paper has been supported by the National Academy of the National Guard of Ukraine (research project No. DR 0124U003278).

References

[1] *Unmanned Systems Roadmap: 2007-2032* [online]. Washington: Department of Defense, 2007 [viewed 2025-02-09]. Available from: https://surl.li/wxhtwy

[2] *Air Target. Power of Precision* [online]. [viewed 2025-02-09]. Available from: https://surl.li/grkggl

[3] VOLYNETS, V.L., N.L. MAMONOVA and O.V. NELSON. Comparative Analysis of Passive Means of Simulating the Radar Cross Section of Air Targets (in Ukraine). *Collection of Scientific Works of the State Research Institute of Aviation,* 2014, **10**(17), pp. 66-71. ISSN 2786-4839.

[4] BOR, J., O. LAFOND, H. MERLET, P. LE BARS and M. HIMDI. Foam Based Luneburg Lens Antenna at 60 GHz. *Progress in Electromagnetics Research Letters,* 2014, **44,** pp. 1-7. DOI 10.2528/PIERL13092405.

[5] CHANGSHENG, D., C. ZIQING, L. YONG, W. HAIDONG, J. CHAO and Y. SHIWES. Permittivity of Composites Used for Luneburg Lens Antennas by Drilling Holes Based on 3-D Printing Technique. *Journal of Terahertz Science and Electronic Information Technology,* 2017, **15**(4), pp. 646-651. DOI 10.11805/tkyda201704.0646.

[6] LIANG, M., W.R. NG, K. CHANG, K. GBELE, M.E. GEHM and H. XIN. A 3-D Luneburg Lens Antenna Fabricated by Polymer Jetting Rapid Prototyping. *IEEE Transaction on Antennas and Propagation,* 2014, **62**(4), pp. 1799-1807. DOI 10.1109/TAP.2013.2297165.

[7] LARIMORE, Z., S. JENSEN, A. GOOD, A. LU, J. SUAREZ and M. MIROTZNIK. Additive Manufacturing of Luneburg Lens Antennas Using Space-Filling Curves and Fused Filament Fabrication. *IEEE Transaction on Antennas and Propagation,* 2018, **66**(6), pp. 2818-2827. DOI 10.1109/TAP.2018.2823819.

[8] XIN, H. and M. LIANG. 3D Printed Microware and THz Devices Using Polymer Jetting Techniques. *Proceedings of the IEEE,* 2017, **105**(4), pp. 737-755. DOI 10.1109/JPROC.2016.2621118.

[9] FUCHS, B., L. COQ LE, O. LAFOND and S. RONDINEAU. Design Optimization of Multishell Luneburg Lenses. *IEEE Transaction on Antennas and Propagation,* 2007, **55**(2), pp. 283-289. DOI 10.1109/TAP.2006.889849.

[10] KUBACH A., A. SHOYKHETBROD and R. HERSCHEL. 3D Printed Luneburg Lens for Flexible Beam Steering at Millimeter Ware Frequencies. In: *47th European Microwave Conference (EuMC)*. Nuremberg: IEEE, 2017, pp. 787-790. DOI 10.23919/EuMC.2017.8230965.

[11] BALDAUF, J., S.-W. LEE, L. LIN, S.-K. JENG, S.M. SCARBOROUGH and C.L. YU. High Frequency Scattering from Trihedral Corner Reflectors and Other Benchmark Targets: SBR Versus Experiment. *IEEE Transactions on Antennas and Propagation*, 1991, **39**(9), pp. 1345-1351. DOI 10.1109/8.99043.

[12] ZAKER, R. and A. SADEGHZADEH. Passive Techniques for Target Radar Cross Section Reduction: A Comprehensive Review. *International Journal of RF and Microwave Computer-Aided Engineering*, 2020, **30**(11), e22411. DOI 10.1002/mmce.22411.

[13] IVANETS, G., V. VOINOV, S. HORIELYSHEV, A. NAKONECHNYI, M. IVANETS, O. VASILYLEVA and Ye. BASHKATOV. Justification of the Feasibility of Creating Promising Air Targets Based on Luneberg Lenses (in Ukraine). *Bulletin of the National Technical University "KhPI" Series: Engineering and CAD,* 2024, **2**, pp. 60-67. DOI 10.20998/2079-0775.2024.2.07.

[14] DSTU EN 62431:2022, *Reflectivity of Absorbers of Electromagnetic Waves of Millimeter Frequency. Measurement Methods* [online]. [viewed 2025-02-09]. Available from: https://online.budstandart.com/ua/catalog/doc-page.html?id_doc=101852

[15] SAYANSKIY, A., S. GLYBOVSKI, V. AKIMOV, P. BELOV and I. MESHKOVSKIY. Broadband 3D Luneburg Lensen Based on Met-Amaterials of Radially Diverging Dielectric Rods. *IEEE Antennas and Wireless Propagation Letters,* 2017, **16**, pp. 1520-1523. DOI 10.1109/LAWP.2016.2647383.

[16] BOGOSLAVETS, S.O., B.Yu. NAUMENKO and O.B. LUZHBINA. Technical Outline of an Air Target in the Interests of the Air Force of the Armed Forces of Ukraine (in Ukraine). *Collection of Scientific Works of the State Research Institute of Aviation,* 2022, **18**(25), pp. 14-19. DOI 10.54858/dndia.2022-18-2.

[17] PANCHENKO, B.A., D.V. DENISOV, V.V. MOKHOVA and R.I. PANOV. Influence of the Stratification Level of the Luneberg Lens on Its Antenna Characteristics. *News of Higher Educational Institutions of Russia, Radioelectronics*, 2014, **1**, pp. 3-6. ISSN 1993-8985.

[18] MALKIN, A.I. and N.S. KNYAZEV. Dielectric Permittivity and Permeability Measurement System. *REIT* [online], 2017, **1814**, pp. 45-51 [viewed 2025-02-09]. Available from: https://ceur-ws.org/Vol-1814/paper-06.pdf

[19] MOZHAROV, E.O. and N.K. GALKIN. Calibration of a Broadband Test Bench for Measuring the Scattering Characteristics of Objects. *Journal of Radio Electronics,* 2018, **10**. DOI 10.30898/1684-1719.2018.10.11.